
Article:
Clarke, S.D., Fay, S.D., Warren, J.A. et al. (2014) A large scale experimental approach to the measurement of spatially and temporally localised loading from the detonation of shallow-buried explosives. Measurement Science and Technology, 26. 015001. ISSN: 0957-0233

https://doi.org/10.1088/0957-0233/26/1/015001

A large scale experimental approach to the measurement of spatially and temporally localised loading from the detonation of shallow-buried explosives

S. D. Clarke[1], S. D. Fay[1,2], J. A. Warren[1,2], A. Tyas[1], S. E. Rigby[1] & I. Elgy[3]

[1]Department of Civil & Structural Engineering, Sir Frederick Mappin Building, Mappin Street, Sheffield, UK, S1 3JD

[2]Blastech Ltd, The Sheffeld Bioincubator, 40 Leavygreave Road, Sheffeld, UK, S3 7RD

[3]Physical Protection Group, Defence Science and Technology Laboratory, Porton Down, Salisbury, UK

E-mail: sam.clarke@sheffield.ac.uk

Abstract.

A large scale experimental approach to the direct measurement of the spatial and temporal variation in loading resulting from an explosive event has been developed. The approach utilises a fixed target plate through which Hopkinson pressure bars are inserted. This technique allows the pressure-time histories for an array of bars to be generated, giving data over a large area of interest. A numerical interpolation technique has also been developed to allow for the full pressure-time history for any point on the target plate to be estimated and hence total imparted impulse to be calculated. The principles underlying the design of the experimental equipment are discussed, along with the importance of carefully controlling the explosive preparation, and the method and location of the detonation initiation. Initial results showing the key features of the loading recorded and the consistency attainable by this method are presented along with the data interpolation routines used to estimate the loading on the entire face.

Keywords: Buried Charges; Impulse, Spatial & Temporal Variation; Hopkinson Pressure Bar; Geotechnics.

1. Introduction

With the increasing use of buried improvised explosive devices in current conflict zones, the quantification of the loading and structural deformation occurring when a shallow buried charge is detonated and the resulting products interact with a target at a small distance above ground level has received considerable attention. This has led to a need for a deeper understanding of the magnitude and mechanisms of load transfer in these explosive events. Being able to design protective structures to withstand such events

and save lives depends on the accurate assessment of the blast loading produced by the detonation of such shallow-buried explosives.

Past phenomenological studies have concentrated on the assessing the deformation caused to a structural target [1, 2, 3]. While this is useful for protective system design and validation purposes, and for gaining some insight into the mechanics of load transfer and structural response, it fails to directly assess the local magnitude and distribution of loading, or the mechanisms by which load is transmitted to the structure. Most direct load measurement studies have concentrated on quantifying the impulse imparted to a target, which is typically spatially integrated over the entire target face [2, 4, 5, 6, 7, 8, 9].

Experimental research into the characterization of blast loading specifically from buried explosives has typically involved a relatively poor control of the geotechnical conditions prior to the blast. This has resulted in highly inconsistent results becoming the accepted norm (it is not uncommon to see scatter of $\pm 15\%$ from nominally identical tests [5]). With careful control it has been shown previously that this can be reduced to $\pm 3\%$ [10] allowing more robust conclusions to be drawn as to the driving mechanisms. As an alternative, some research groups remove the blast-related aspects altogether by using well controlled small scale laboratory samples loaded by compressed gas [11]. This approach has the drawback of over-simplifying the problem by ignoring the air-shock, geometrical and thermal aspects of the loading, and perhaps even more critically concentrating only on the sand throw as the mechanism for impulse transfer.

1.1. Experimental considerations

The most fundamental issue in determining the experimental methodology for recording loading from any blast-related event, is accurate characterisation of the conditions at the point of load measurement. This comes down to a decision on whether to attempt to sample the free-field pressures with non-invasive instrumentation which does not affect the flow of the shock and/or particles, or whether to have a barrier at the point of load measurement, and record the pressure generated by the reflection of the shock and/or particles. In air-shock loading, attempts can be made to capture something approaching free-field pressure by the use of side-on pressure gauges in profiled mounts, or small 'pencil-gauges' [12, 13]. Some inconsistency persists on whether these measurements truly are non-invasive, and large variations in loading from nominally identical tests have been reported [14]. In the current authors' experience, measurements of reflected blast pressures from effectively rigid targets is a simpler task, offering better characterised conditions and a high degree of test-to-test repeatability [15, 16].

In loading from a shallow-buried explosive charge, the nature of the loading will potentially be influenced by the reflection of both air shock and soil particles. The magnitude and duration of loading will be affected by compliance of the loaded target, although compliance effects may be negligible if the loading is highly impulsive (i.e. the loading is substantially completed before the target has deformed significantly).

For the current work, it was decided that the most suitable approach was to

effectively eliminate the issue of target compliance, by introducing an extremely stiff barrier as the target, and consequently, to record the fully reflected loading. Further, it was decided to make the target sufficiently wide that any pressure relief generated by clearing or flow around the target edge [17, 18, 19] would be of minor importance, at least in the early stages of very high loading magnitude. These decisions mean that the boundary conditions are well characterised, and loading measurements are an upper bound on the actual loading that a small-sized or highly compliant target might experience.

1.2. Instrumentation considerations

There are a range of instrumentation techniques which can be utilised to capture the spatial and/or temporal distribution of load. These are summarised in Table 1.

Table 1. Possible instrumentation types for capturing the spatial and/or temporal distribution of load

Scheme	Duration of load recording	Temporal resolution	Spatial resolution	Min load resolution	Moving / fixed target	Robustness	Ease of implementation	Cost
Hopkinson pressure bars	✓(≈1 ms)	✓✓✓	✓✓✓	✓(≈1MPa)	✓(F)	✓✓✓	✓✓✓	✓✓
Stress gauge	✓✓✓(∞)	✓✓✓	✓✓	?	✓✓(F/M)	✓	✓✓	✓
Piezo-electric/ resistive pressure gauge	✓✓✓(∞)	✓✓✓	✓✓	Varies	✓✓(F/M)	✓	✓✓	✓
Impulse/ momentum traps	✓✓✓(∞)	✓	✓	Varies	✓✓(F/M)	✓✓✓	✓✓✓	✓✓✓
Load cells	✓✓✓(∞)	✓	-	Varies	✓(F)	✓✓✓	✓✓✓	✓✓✓

Based on previous studies conducted [20, 21] an indicative pressure-time history was developed to enable the assessment of possible instrumentation scenarios. The pressure trace shown in Figure 1 consists of four distinct phases; (a) an initial pre-cursor load, (b) a very high magnitude, short duration 'shock' pressure ($\gg$100 MPa magnitude, $\ll$1 ms duration), (c) a post-peak load plateau and a rapid fall to, (d) a low magnitude, but long duration 'stagnation pressure' which may comprise a significant proportion of the total impulse from the loading. Due to the requirement to measure both the shock and stagnation pressures, a decision was made to use multiple instrumentation types; Hopkinson pressure bars (HPBs) to capture the short duration loading, backed

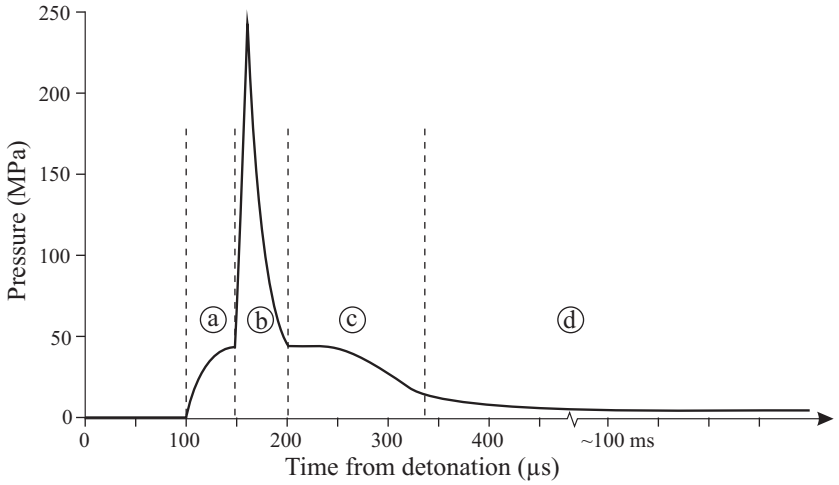

Figure 1. Indicative pressure-time history for instrumentation regime [20, 21]

up by load cells to measure the overall impulse. The use of these instrumentation types enforced the use of the fixed plate approach in the overall experimental design.

1.3. Preliminary numerical studies

Initial numerical simulations were also conducted to determine if the long duration loading would influence the deformation of a 'typical' deformable target, and hence require accurate quantification. A 12.5 mm thick, 500 mm square plate with full translational and rotational constraint along all four edges, was modelled using LS-DYNA [22] under a uniformly applied load, based on the indicative pressure-time history outlined previously, which is presented in Figure 2. The influence of the long duration, low magnitude feature of the load was evaluated by simulating target response to a tail pressure, p_{tail}, of 0, 1, 2 and 5 MPa. The total load duration was set to 10 ms.

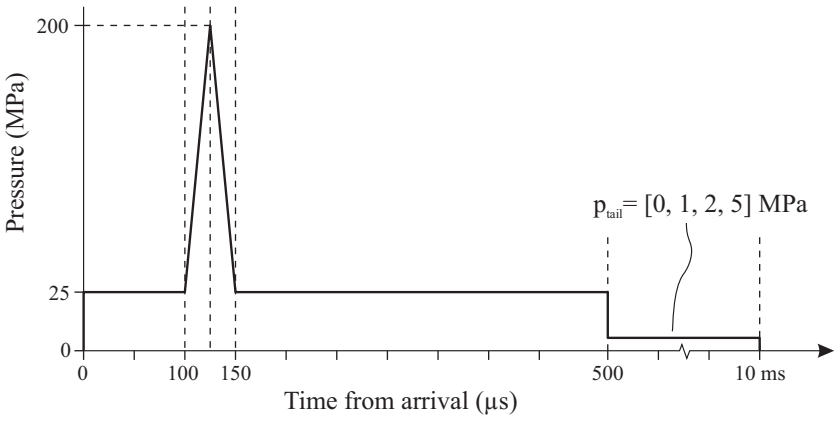

Figure 2. Simplified pressure-time history for numerical simulations

The plate was modelled as a linear-elastic perfectly-plastic material with density, Young's modulus, Poisson's ratio and yield stress of 7850 kg/m^3, 210 GPa, 0.3 and

300 MPa respectively. A summary of the peak numerical displacements is shown in Table 2.

Table 2. Summary of peak numerical displacements from the preliminary study of a 500 mm square, 12.5 mm thick fully clamped plate representing a 'typical' deformable target

p_{tail} (MPa)	Pre-tail impulse (Ns)	Tail impulse (Ns)	Peak displacement (mm)	% displacement increase from tail
0	4.22	0.00	172.4	-
1	4.22	2.38	176.0	2.1
2	4.22	4.75	179.5	4.1
5	4.22	11.88	193.0	11.9

It can be seen that the tail pressure has a relatively low impact on the peak displacement of the plate. For the highest magnitude tail pressure, the impulse associated with the tail is 74% of the total impulse, yet this only accounts for a 12% increase in peak displacement. It can be concluded, therefore, that the primary function of the instrumentation should be to accurately quantify the high magnitude, short duration features of the load on account of the greater impact on target deformation, justifying the instrumentation choice. Further numerical analyses were also run using a non-uniform loading focussed on the centre of the plate but this was seen to have a minor influence on the trends seen in Table 2.

2. Experimental setup

2.1. Scaling

The first decision to be made regarding the experimental setup was the scale at which to conduct the experiment. To remove environmental factors one requirement of the experimental programme was that it should be conducted indoors, in a partially buried concrete bunker structure at the University of Sheffield Blast & Impact Laboratory (maximum charge rating: 500 g TNT equivalent). It was also required that the experiment should be conducted at as small a scale as possible whilst allowing a controllable burial depth when using sub-surface charges. The NATO standard for buried charge testing [23] specifies a burial depth of 100 mm in full scale tests. With very shallow depths <20 mm, the soil overburden would be very difficult to control.

To allow for extremely tight control over the soil bed and to be compatible with the explosives engineering implications, 1/4 scale tests have been opted for. This lowers the amount of material required in each test (the size of the soil container is directly proportional to scale) while giving a controllable burial depth (25 mm). At 1/4 scale the charge size required to scale down a full scale 5 kg charge is 78 g.

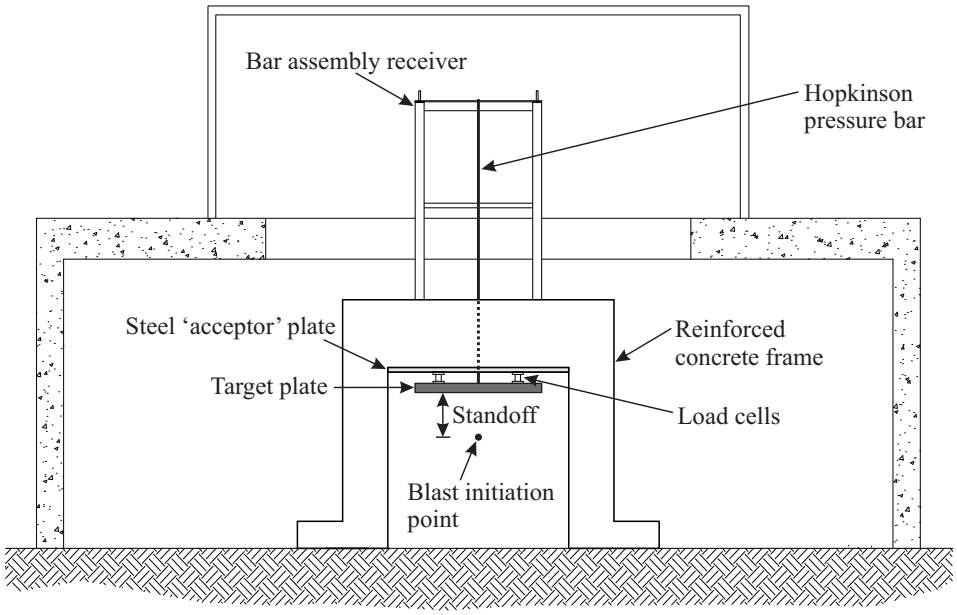

Figure 3. Schematic of the test frame

2.2. Test frames

The experimental setup is based around two large, specifically fabricated test frames. The frames are constructed from fibre and steel reinforced concrete (500 mm square columns with a 750 mm deep, 500 mm wide beam spanning the columns) shown in Figure 3. Cast into the lower face of each of the beams is a 50 mm thick steel plate (the acceptor plate) which serves two purposes; to shield the concrete from the blast and associated fragmentation, and also to allow for further instrumentation to be easily affixed. Four load cells are attached to the acceptor plate to which the target plate is fixed. The target plate is a 1400 mm diameter, 100 mm thick mild steel plate. Initial numerical simulations were also utilised to check that the target plate would not deflect noticeably when subjected to the blast pressures estimated – a 100 mm thick, 1400 mm diameter plate (with boundary conditions approximately representing those of the test rig, i.e. full translational and rotational constraint at nodal locations corresponding to parts of the plate in contact with the load cells) was evaluated under LS-DYNA [22] routine *LOAD_BLAST [24] (100 g at 75 mm free air spherical blast). The peak displacement was less than 0.3 mm.

2.3. Instrumentation

Whilst the use of HPBs as the primary means of recording the expected high magnitude, short duration initial loading has several advantages (robustness, high load capacity) it is important to discuss issues which should be taken into account in interpreting the HPB results.

Firstly, the duration of load that can be recorded using a HPB is limited by the

time taken for the elastic stress pulse to reach the distal end of the bar and return to the strain gauge station close to the proximal face of the bar. After this time, the strain gauge station records a superposition of any still-incoming load and reflections of the earlier stages of the loading pulse. In the current work, the bars were chosen to be 3.25 m long, and with the strain gauge station set 0.25 m from the loaded face of the bar, this gives a total load record duration of ∼1.2 ms before the arrival of the reflection from the distal end.

A more problematic issue in HPB use is that propagating waves in a HPB experience dispersion due to the fact that the propagation velocity in the bar is a function of the frequency of each Fourier component of the loading. As a recording station on the bar is typically several bar diameters from the loaded face of the bar (in this case, to enable the strain gauge station to be positioned above the steel target plate and thus be protected from the air shock/particle barrage loading) dispersion may mean that the recorded signal differs significantly from the actual load applied to the bar face. The practical effects of dispersion are that loading features with timescales of the order of a few microseconds are difficult to determine from the dispersed loading record, and the dispersed signal typically displays several characteristic forms of oscillation, due to the phase shift in the Fourier components. Whilst it is possible in principle to correct for dispersion effects, using frequency domain phase-shift methods developed in the 1980s [25, 26], Tyas & Watson [27, 28] demonstrated that there is a currently a practical upper bound to the frequency range over which these can be applied, limiting the bandwidth of a steel HPB to around $1250/a$ kHz, where a is the bar radius in mm. There is thus a benefit to using bars of as small a radius as practically possible. In the current work, a radius of 5 mm was chosen, giving an effective bandwidth of ∼250 kHz.

A single bar is able to give the pressure-time history of a single point. To obtain pressures over a given region an array of HPBs can be used to give the pressures at multiple locations at any given time. When designing the target plate the degree of spatial variance of pressure was unknown, hence the target plate was pre-drilled with a hole arrangement which would allow variations in the spacings of the HPB array, shown in Figure 4. The bars are a close fit to the holes drilled in the target plate whilst giving sufficient tolerance to prevent coupling of the bars with any deformation and flexure of the target plate. The bottom end of the HPBs lies flush with the blast face of the target plate with the top end of the HPBs being held in place vertically by a receiver frame placed atop the main reaction frame (Fig. 3). The HPBs are suspended by their top ends so that they are free to displace vertically upwards during the loading period, coming to rest again on the receiver frame post test. An initial series of commissioning testing indicated that foil strain gauges were prone to signal noise, possibly caused by ionisation from the detonation products. Semiconductor strain gauges were therefore used, with the benefit of increased output and reduced signal noise.

To give a measure of the total integrated pressure-time history, loads cells have been used to connect the target plate to the reaction frame. Load cells are effectively equivalent to impulse traps, with the displacement of the distal face of the gauge

restrained by the reaction frame. A short length of measurement block will then experience axial stress which is effectively uniform along its length, and which can be recorded by strain gauges. The temporal resolution of this type of gauge is related to both its length (i.e. the stress wave propagation time along the gauge) and the vibration characteristics of the reaction frame, but with careful design should be of the order of a few hundred microseconds, making it suitable for long-term cumulative impulse measurement, but potentially not suitable for temporally resolving the short duration pressure spike. The recording duration of this instrumentation is effectively infinite. Data was recorded using TiePie Handyscope 16-Bit Digital Oscilloscopes, with isolated inputs for each channel (HPBs, load cells and breakwire). Signal conditioning and amplifiers were combined into a single unit with differential circuits

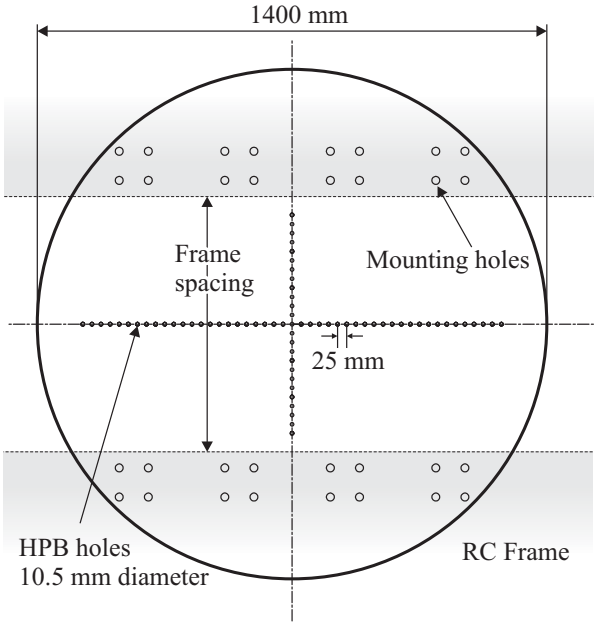

Figure 4. Detail of the target plate instrumentation arrangement

2.4. Detonation initiation

With the developed methodology capable of measuring the pressure distribution from both free air and buried charges, thought had to be given to the detonation method. Initial tests were conducted with a top detonated charge, while this was seen to show the expected characteristics (Fig. 1) there was a large degree of noise in the data as well as large variations from test to test. An example of the top detonated pressure-time history for the central HPB (directly above the charge) is shown in Figure 5. The detonation study was conducted on preliminary shallow buried cylindrical explosives, with further detail available in Ref. [29].

There were concerns regarding top detonation, with the command line exiting the surface of the soil directly above the charge (due to shallow burial and detonator length). This was thought to give a preferential path for venting the detonation pressures, whilst

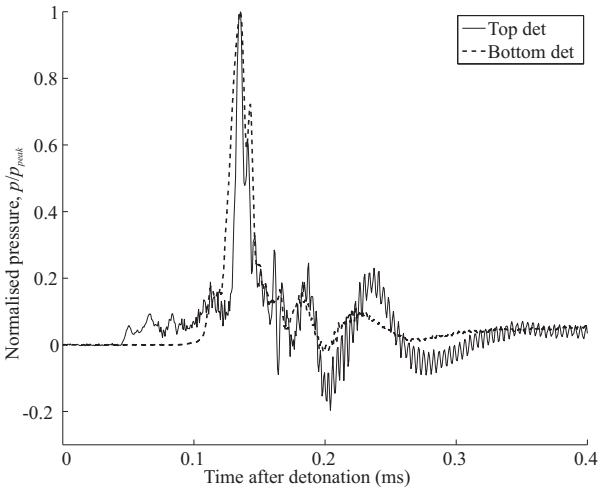

Figure 5. Comparison of detonator arrangements in buried charge tests

contact of the breakwire with the target face could have introduced the high degree of noise seen in the data. Bottom detonation was therefore investigated.

For safety reasons, when combining the detonator and charge, precautions must be taken so that the detonator cannot be initiated by accidental or deliberate means. In buried charge tests, the burial process for a bottom detonated charge leaves the firing officer exposed for approximately 15 minutes. Furthermore the soil bin must be located in the trial apparatus. Non-el (non-electric) detonators can only be triggered by a fire set which is kept on the person of the firing officer. To remove the potential for accidental initiation of electrical detonators, non-el detonators were therefore used to initiate the base detonated charges.

Figure 5 also shows the central HPB trace for the base detonated charge. Here the arrival of the shock is much cleaner, with a reduced duration pre-cursor load and reduced electrical noise. Two things should be noted here: 1) due to the strong directionality of the detonators, laterally detonated charges were not considered and 2) the traces shown in Figure 5 have been normalised by peak pressure and time shifted so that the peak pressure and arrival times are the same to allow for a direct phenomenological comparison. Whilst the amount of explosive in both the top and bottom detonated experiments was the same, the directionality of the detonation made a large difference to the magnitude of the peak pressures.

2.5. Free air tests

To ensure that the traces recorded by the HPBs were accurate representations of the known blast pressures, the semi-empirical weapon effects estimation tool, ConWep [30], was used to predict the pressures for a 100 g spherical PE4 free air blast detonated at a normal distance of 75 mm from the central bar, shown in Figure 6b. 5 bars were used in the array, with one central bar and 4 radial bars at 100 mm away from the centre of the plate. It can be seen in Figure 6a that there is a high degree of agreement with the peak

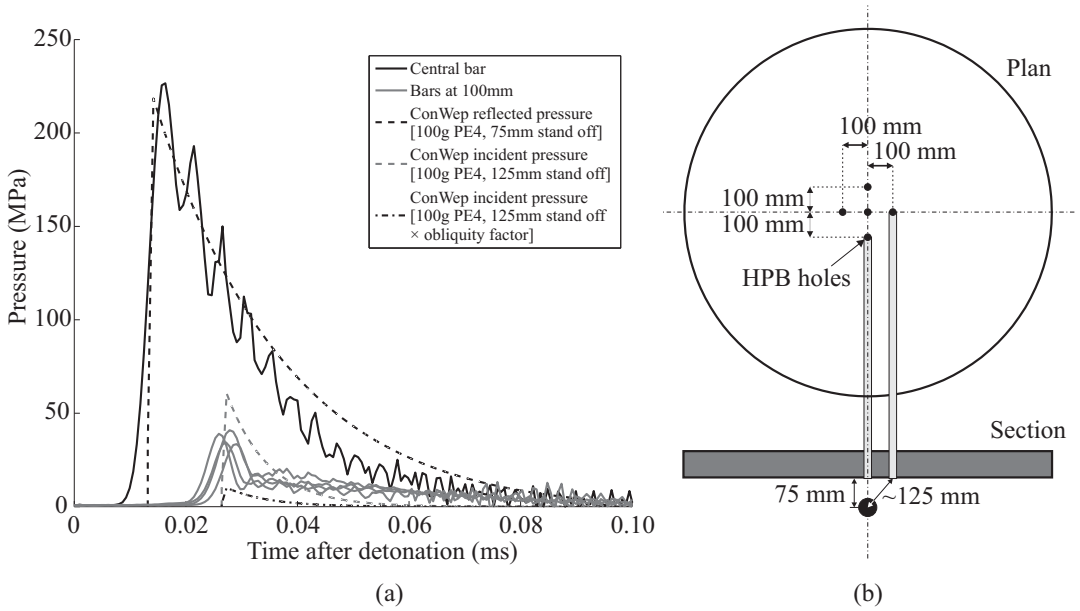

Figure 6. a) Comparison of measured traces against ConWep predictions, b) Charge mass, stand-off and bar array used in the experiment

normally reflected pressure for the central bar. The radial bars at 100 mm also showed good agreement with the 125 mm ConWep oblique reflected pressure (incident pressure multiplied by obliquity factor), with the shock travel time between central and radial bars also being accurately measured. The oscillations in the HPB signals are known to be caused by dispersion, which for the purposes of this paper has not been accounted for.

Figure 7 shows the total reaction force from the load cell data for 3 separate free air tests, again using 100 g PE4 detonated at 75 mm normal stand-off. The reaction force data contains components of both the applied force and the dynamic reaction force caused by oscillations of the plate, load cells, and frame, so cannot be immediately used to quantify the impulse imparted to the plate from the blast. What is clear, however, is that the reaction force data, and hence the applied force, displays excellent repeatability from test to test and gives confidence that the test parameters are being adequately controlled. The reaction force data can therefore be primarily used as a tool to verify that the outcome of the experiment is as expected.

3. Numerical interpolation

3.1. Interpolation for a 1D HPB array

With the HPBs giving data for specific points over the target plate, an interpolation routine was developed to infer the pressure time history for any point on the plate and hence quantify the total impulse delivered. With the data for different bars being separated in both space and time, a two part interpolation was used which was designed

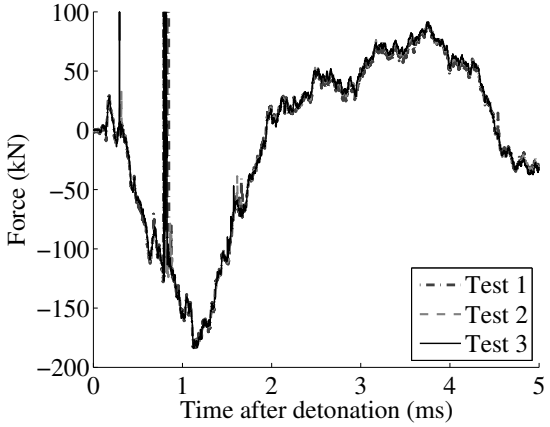

Figure 7. Reaction force-time history for free air tests

to be able to cater for any arrangement of HPBs in the target plate. A contour plot of the measured HPB array data for a single radial direction (x) is shown in Figure 8a. It can be seen that the data from the HPBs is discontinuous making a true 2D interpolation impossible. The 3 stages in the interpolation routine are shown in Figure 8b-d. The first stage of the interpolation was to time-shift all data in each radial direction so that the peak pressure for each bar arrives at the same time as the peak pressure of the central bar, which is the only bar common to each radial direction (Eq. 1). This assumes that for each pressure trace there is a single well-defined pressure spike which corresponds with the arrival of the shock front.

$$\Delta t = t_{p_{peak}} - t_{p_{peak,0}} \tag{1}$$

An example of the time-shifted data is seen in Figure 8b where the variation in pressure with radial distance and time can clearly be seen. Estimating the pressure at 40 mm at a time of 0.025 ms directly from Figure 8a would give a pressure around 0. In the interpolation routine, the pressure at any radial distance is interpolated from Figure 8b with the data then time-shifted to fit the shock front arrival times as indicated in Figure 8c. The arrival times are calculated form the original time-shift equation (Eq. 1). The interpolated pressure and time-shifted data is shown in Figure 8d where the continuous shock data can clearly be seen. It is recommended that a separate interpolation routine is performed on test data captured from each experiment. Using a combination of test data from different experiments introduces the risk of test-to-test variability corrupting the interpolation.

The interpolation process described thus far is capable of giving the pressure-time history for any point on the target plate assuming axi-symmetric conditions from a single direction of radial HPBs. The main issue with this method of interpolation is that if the detonation is not axi-symmetric and coaxial with the HPB array the data gathered may underestimate the loading. To overcome this limitation the pressures can be measured by an array in each radial direction (x, y, $-x$, $-y$). Leading to the requirement for the

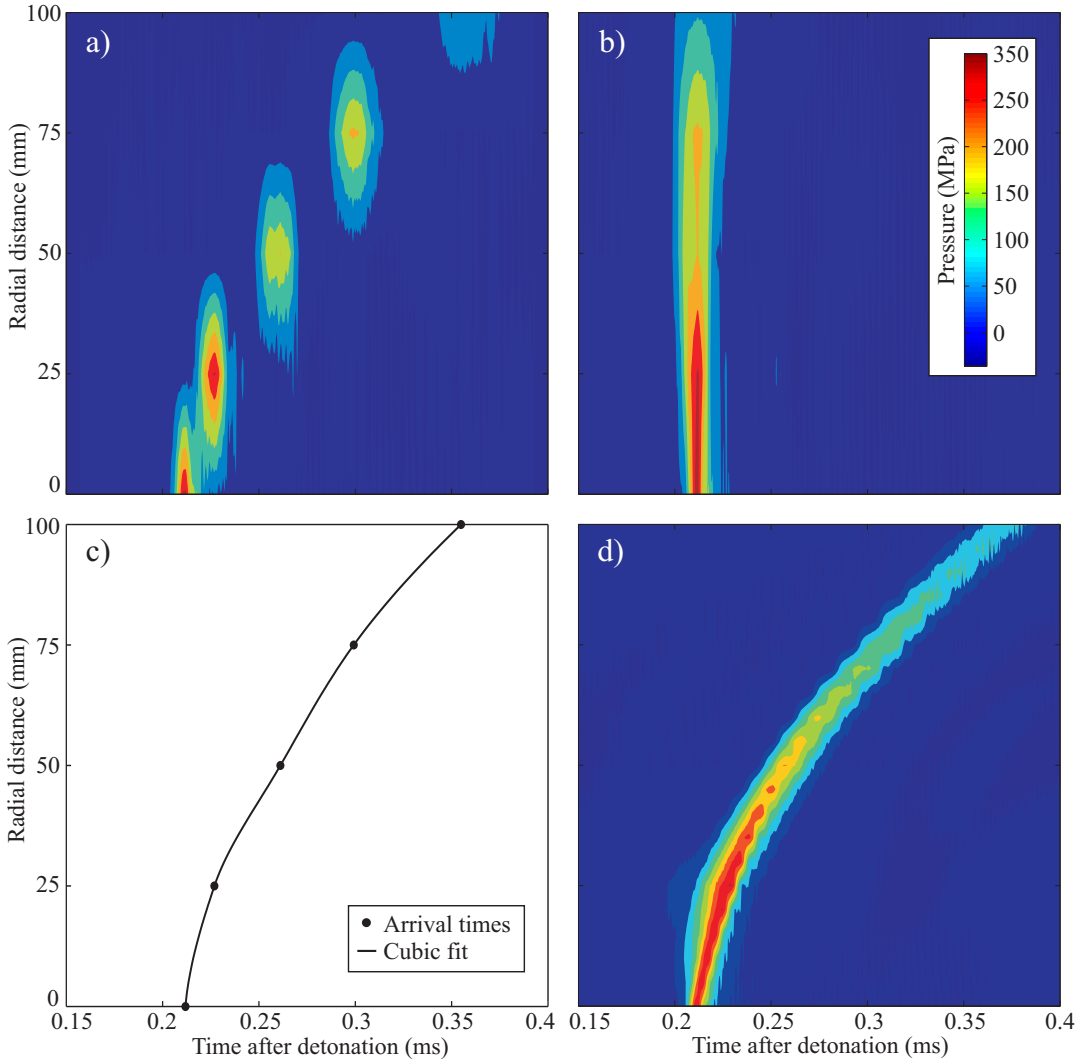

Figure 8. Interpolation sequence for 1D HPB array a) original data, b) time-shifted data, c) shock front arrival times and d) final interpolated pressure time data

interpolation to be able to generate the pressure time history for the target plate from a full (4 directional) array of HPBs.

3.2. Interpolation for a 2D HPB array

With a full 2D array of HPBs the pressure at any point is no longer simply related to the radial distance, but rather the radial distance and the angular rotation, as illustrated in Figure 9a. The original data for a single radius ($r = 50$ mm) is shown in Figure 9b. As for the single array interpolation the arrival time for the shock front at each HPB is used to time-shift the data so that the shock fronts all align. This then allows the pressure at any angular rotation, θ, to be calculated by using a linear interpolation on the aligned data (Fig. 9c). In the data array for interpolation the x axis array is repeated at 0° and 360° to simplify the interpolation. The full 2D interpolation of pressure is achieved through the following process;

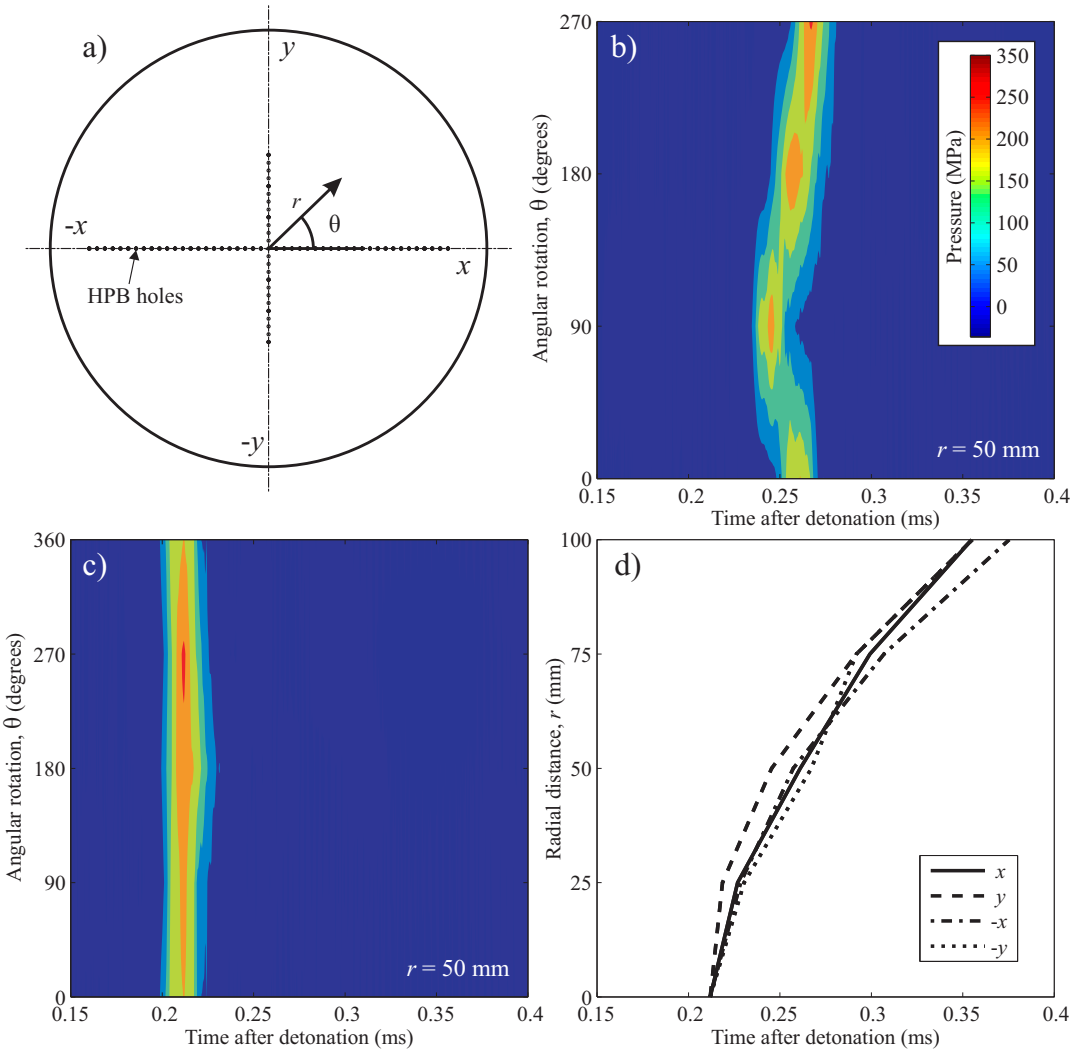

Figure 9. Interpolation sequence for 2D HPB array a) sign conventions used, b) original data $r = 50$ mm, c) time-shifted data $r = 50$ mm, and d) arrival times for each radial direction.

(i) time-shift all HPB pressure traces by Δt (Eq. 1),

(ii) calculate r and θ for point of interest,

(iii) apply the 1D interpolation to HPB arrays closest to the point of interest for known r (for θ=45° the interpolation would use the x and y arrays),

(iv) interpolate linearly between the 2 pressures based on θ,

(v) repeat for all locations and times,

(vi) time-shift the pressure time history for each location based on cubic interpolation of the shock arrival time (Fig. 9d).

The interpolated pressure distributions over a 100 × 100 mm area of interest (5 mm grid) for selected times are shown in Figure 10. The original data was measured using a 17 HPB array (5 in each radial direction with 25 mm spacings). The test configuration

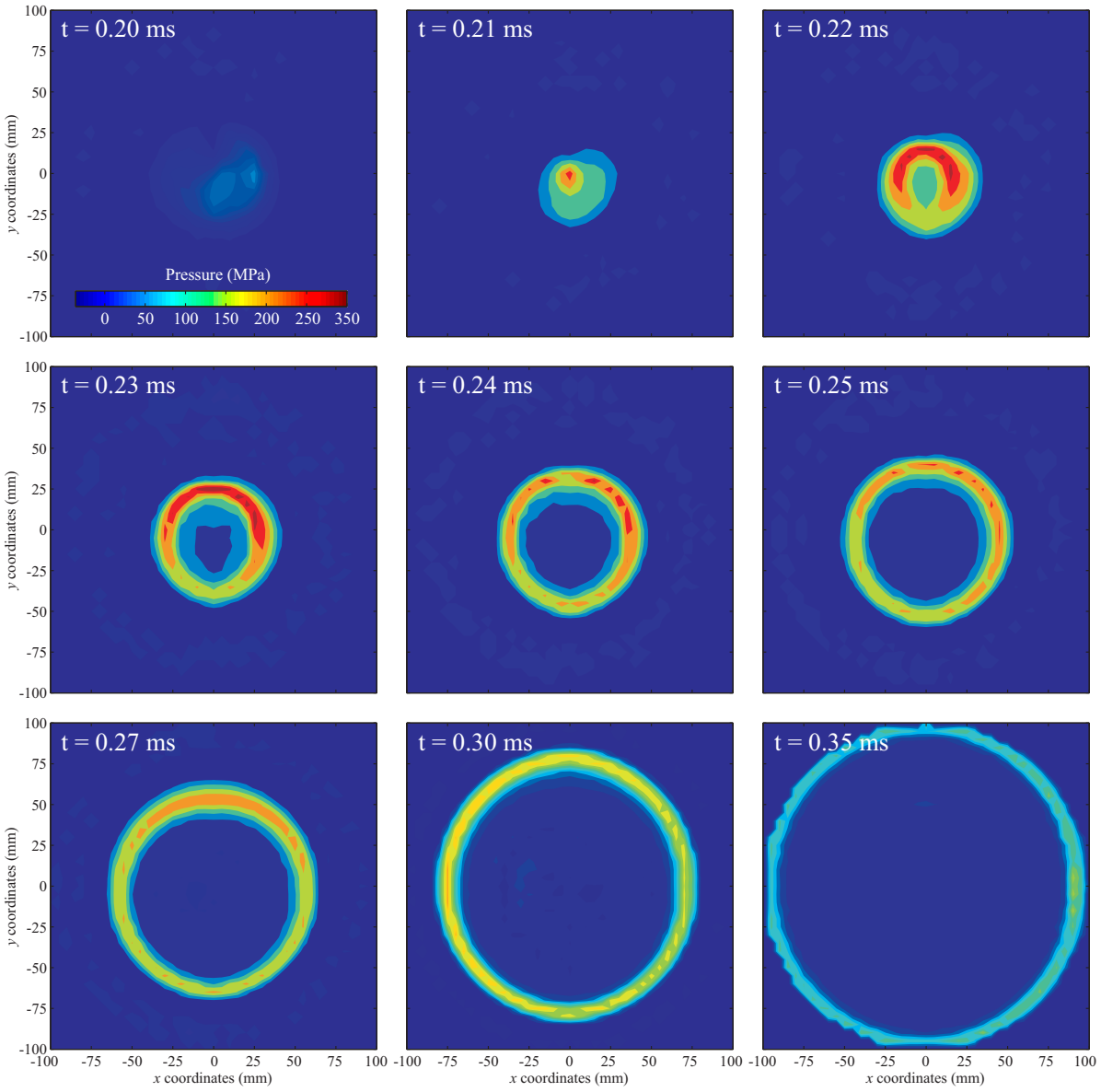

Figure 10. Interpolated pressure distribution plots at specified times

was a 78 g PE4 charge buried at 28 mm in a saturated fine sand [31, 32] with a 140 mm stand off. The asymmetric nature of the loading can be seen at all times, with the shock front being continuous throughout. The time origin t=0 is that of the charge detonation, with there being ≈20 ms travel time to the target plate. As the interpolation runs for all grid locations, multiplying each interpolated pressure by the element area gives the load on any grid location. Multiplying this load by the time interval and then summing for all times and locations gives the total impulse acting on the target plate.

It is worth noting that the interpolation routine cannot allow for localised particle strikes that occur outside of the areas populated by the Hopkinson pressure bars. Unless the particle strike causes rupture, the effect is unlikely to influence peak target deformation and the measurement technique described in this paper is adequate for

capturing the primary features of near-field and shallow buried blast loading.

4. Conclusions

A large, 1/4 scale experimental approach has been developed which, through the combined use of a rigid reaction frame and Hopkinson pressure bars, is capable of resolving the spatial and temporal distribution of loading from explosive charges. The experiment has been designed to measure blast pressures from both free-air and buried charges. Initial testing of the approach showed the importance of carefully considering the directionality of the detonation when using buried charges, with top detonated charges introducing spurious data in the form of a pre-cursor load. The free-air pressure time histories have been compared with commensurate predictions from ConWep which show a high degree of agreement and hence give confidence in the accuracy of the method. The load cells fitted to the rigid target plate have also been used to quantify any test to test variation in impulse from the charges. This comparison has showed that for 3 nominally identical free air tests the measured load-time history was identical, giving confidence that there is almost no variability in the explosive (PE4) and that a repeatable stable detonation can be achieved at 1/4 scale.

Finally, a method has been presented for the interpolation of pressure time histories over an area of interest from a discrete array of Hopkinson pressure bars. It has been shown for both 1D and 2D Hopkinson pressure bar arrays the interpolation leads to feasible estimations of the shock front arrival time and associated pressures. The interpolation routine works on a pre defined grid, generating pressure-time histories at each point allow direct application into numerical modelling software.

5. Acknowledgements

The authors wish to thank the Defence Science and Technology Laboratory for funding the published work.

6. References

[1] A Neuberger, S Peles, and D Rittel 2007 Scaling the response of circular plates subjected to large and close-range spherical explosions. Part II: Buried charges *International Journal of Impact Engineering* 34(5) 874–882

[2] E.G. Pickering, S. Chung Kim Yuen, G.N. Nurick, and P. Haw 2012 The response of quadrangular plates to buried charges *International Journal of Impact Engineering* 49 103–114

[3] Shaowen Xu, Xiaomin Deng, Vikrant Tiwari, Michael a. Sutton, William L. Fourney, and Damien Bretall 2010 An inverse approach for pressure load identification *International Journal of Impact Engineering* 37(7) 865–877

[4] Bergeron D M and Trembley J E 2000 Canadian research to characterize mine blast output *16th Int. Sym. on the Military Aspects of Blast and Shock, Oxford, UK*

[5] Hlady S L 2004 Effect of soil parameters on landmine blast *18th Int. Sym. on the Military Aspects of Blast and Shock, Bad Reichenhall, Germany*

[6] Fourney W L, Leiste U, Bonenberger R and Goodings D J 2005 Mechanism of loading on plates due to explosive detonation *Int. J. on Blasting and Fragmentation* 9(4) 205–217
[7] Anderson C E, Behner T and Weiss C E 2011 Mine blast loading experiments *Int. J. of Impact Eng.* 38(8-9) 697–706
[8] Fox D M, Huang X, Jung D, Fourney W L, Leiste U and Lee J S 2011 The response of small scale rigid targets to shallow buried explosive detonations *Int. J. of Impact Eng.* 38(11) 882–891
[9] Akers S A Ehrgott J Q, Rhett R G and Rickman D D 2011 Design and fabrication of an impulse measurement device to quantify the blast environment from a near-surface detonation in soil *Experimental Techniques* 35(3) 51–62
[10] Clarke S D, Warren J A and Tyas A 2011 The influence of soil density and moisture content on the impulse from shallow buried explosive charges *Int. Sym. on Interaction of the Effects of Munitions with Structures, Seattle, US*
[11] McShane G J, Deshpande V S and Fleck N A 2013 A laboratory-scale buried charge simulator *Int. J. of Impact Eng.* 62 210–218
[12] Netherton M D and Stewart M G 2013 The variability of blast-loads from military munitions and exceedance probability of design load effects *15th Int. Sym. on the Interaction of the Effects of Munitions with Structures* Potsdam, Germany
[13] Spranghers K, Vasilakos I, Lecompte D, Sol H and Vantomme J 2012 Full-field deformation measurements of aluminum plates under free air blast loading *Experimental Mechanics* 52(9) 1371–1384
[14] Netherton M D and Stewart M G 2010 Blast load variability and accuracy of blast load prediction models *Int. J. of Protective Structures* 1(4) 543–570
[15] Tyas A, Warren J, Bennett T and Fay S 2011 Prediction of clearing effects in far-field blast loading of finite targets *Shock Waves* 21(2) 111–119
[16] Rigby S E, Tyas A, Bennett T, Clarke S D and Fay S D 2014 The negative phase of the blast load *Int. J. of Protective Structures* 5(1) 1–20
[17] Rigby S E, Tyas A and Bennett T 2012 Single-degree-of-freedom response of finite targets subjected to blast loading - the influence of clearing *Engineering Structures* 45 396–404
[18] Rigby S E, Tyas A, Bennett T, Warren J A and Fay S 2013 Clearing effects on plates subjected to blast loads *Engineering and Computational Mechanics* 166(3) 140–148
[19] Rigby S E, Tyas A and Bennett T 2014 Elastic-plastic response of plates subjected to cleared blast loads *Int. J. of Impact Eng.* 66 37–47
[20] Taylor L, Fourney W, Leiste U and Cheeseman B 2008 Loading mechanisms from shallow buried explosives *University of Maryland presentation*
[21] Tyas A 2010 Experimental studies of direct pressure measurement of loading from shallow buried explosive charges, BT-DPD-055 *Technical Report issued to DSTL, Porton Down*
[22] Hallquist J O 2006 LS-DYNA theory manual *Livermore Software Technology Corporation, CA, USA*
[23] NATO 2006 Procedures for evaluating the protection level of logistic and light armoured vehicles *Allied Eng. Publication (AEP) 55* Vol.2 (for Mine Threat)
[24] Randers-Pehrson G and Bannister K A 1997 Airblast loading model for DYNA2D and DYNA3D *U.S Army Research Laboratory, Aberdeen Proving Ground, MD, USA* (ARL-TR-1310)
[25] Follansbee P S and Frantz C 1983 Wave propagation in the split hopkinson pressure bar *J. of Eng. Materials and Technology* 105(1) 61–66
[26] Gorham D A 1983 A numerical method for the correction of dispersion in pressure bar signals *J. of Physics E: Scientific Instruments* 16 477–479
[27] Tyas A and Watson A J 2000 A study of the effect of spatial variation of load in the pressure bar *Measurement science and technology* 11(11) 1539–1551
[28] Tyas A and Watson A J 2001 An investigation of frequency domain dispersion correction of pressure bar signals *Int. J. of Impact Eng.* 25(1) 87–101
[29] S. Fay, S. Clarke, J. A. Warren, A. Tyas, T. Bennett, J. Reay, I. Elgy, and M. Gant Capturing the

spatial and temporal variations in impulse from shallow buried charges In *15th International Symposium on the Interaction of the Effects of Munitions with Structures (ISIEMS)* Potsdam, Germany 2013

[30] Hyde D W *Conventional weapons program (ConWep)* U.S Army Waterways Experimental Station, Vicksburg, MS, USA 1991

[31] Clarke S D, Warren J A, Fay S D, Rigby S E and Tyas A 2012 The role of geotechnical parameters on the impulse generated by buried charges *22nd Int. Sym. on the Military Aspects of Blast and Shock* November 5-9, Bourges, France

[32] Warren J, Kerr S, Tyas A, Clarke S, Petkovski M, Jardine A, Church P, Gould P and Williams A 2013 Briefing: UK ministry of defence force protection Eng. programme *Proceedings of the ICE - Eng. and Computational Mechanics* 166(3) 119–123